3.5 THREE-DIMENSIONAL HIGH-RESOLUTION NATIONAL RADAR MOSAIC

Jian Zhang[1], Kenneth Howard[2], Wenwu Xia[1], Carrie Langston[1], Shunxin Wang[1], and Yuxin Qin[1]

[1] Cooperative Institute for Mesoscale Meteorological Studies, University of Oklahoma, Norman, OK
[2] National Severe Storms Laboratory/NOAA, Norman, OK

1 INTRODUCTION

The National Weather Service (NWS) has implemented the communication infrastructure that facilitates the central collection and distribution of base level data in real time from ~130 WSR-88D (Weather Surveillance Radar – 1988 Doppler) sites to several centralized locations or hubs (http://www.roc.noaa.gov/NWS_Level_2/AMS.asp). End users from government agencies, universities and private industries can access and retrieve the base level data in real-time from the centralized hubs. The National Severe Storms Laboratory, utilizing the communication infrastructure, has instituted a National Mosaic and multi-sensor QPE (Quantitative Precipitation Estimation), or NMQ, system and research program. The NMQ system takes base level data from all available radars at any given time, performs quality control, and then combines reflectivity observations from individual radars onto a unified 3D Cartesian grid that covers the contiguous United States (CONUS). The CONUS 3D radar mosaic grid has a 1-km horizontal resolution over 21 vertical levels with a 5-minute update cycle.

The NMQ 3D reflectivity grid can be used for multi-sensor severe storm algorithms, regional rainfall products generation, aviation weather applications, and data assimilations for convective scale numerical weather modeling. Further, the system provides a national test bed for the development and operational infusion of hydro meteorological techniques. For example, precipitation rate and type will be derived from the 3D mosaic grid in combination with other remote sensing data including satellite, numerical weather prediction models, and lightning. The NMQ system will also produce 1-km resolution hourly to seasonal precipitation accumulations at frequencies of hourly or higher over the CONUS domain. The NMQ CONUS precipitation grid can serve as a verification data set for quantitative precipitation forecasts from numerical weather prediction models. The current paper focuses on the algorithm and the process for the 3-D reflectivity mosaic grid generation.

*Corresponding Author address: Jian Zhang, 1313 Halley Circle, Norman, OK 73069; e-mail: jian.zhang@noaa.gov.

The following section, section 2, provides an overview of the communication and computation infrastructure of the national radar mosaic. Sections 3 and 4 provide a technical description of the mosaic process including radial alignment, reflectivity quality control, single radar data remapping from spherical to Cartesian grid, and multiple radar mosaicing. Example results of the 3D national radar mosaic are also given in section 4. The last section, section 5, provides a summary and a brief introduction for the NMQ project future plans.

2 THE NMQ SYSTEM

An overview flowchart of the NSSL NMQ 3D radar mosaic system is shown in Figure 1. Base level (or "level-2") data from about 130 WSR-88D radars are sent to the University of Oklahoma (OU) -- one of three NWS level-2 data hubs -- utilizing Local Data Management (LDM, http://my.unidata.ucar.edu/content/software/ldm/index.html) compression and across the Internet 2. The use of the LDM compression technique and the Internet 2 communications backbone has assured a very reasonable latency (mostly less than 1 minute) between when data are collected at the radar site and when the data are received by the NSSL NMQ system. The NMQ system receives the level-2 data from the OU radar hub. Once a radar volume scan of data from the radar is fully received, the data are pre-processed for radial alignment, velocity dealiasing, reflectivity quality control, and brightband identification (Fig. 1). All these processes are performed in the native radar (spherical) coordinates. After the quality control, single radar reflectivity data are remapped from their native spherical coordinates to a Cartesian coordinates system. Once remapped the individual radar data are mosaiced for individual geographical tiles across the CONUS. For computation efficiency in addition to utilizing an economic cluster computing architecture, the CONUS domain was divided into 14 regional tiles (Fig. 2) in which multiple radars are mosaiced. Each tile consists of a 3D Cartesian grid in the cylindrical equidistant map projection with a horizontal resolution of 0.01° (longitude) × 0.01° (latitude) over 21 height levels ranging from 1 km to 17 km above mean sea level (MSL). The vertical grid interval is 500 m below 5 km MSL and is 1000 m above it. The final CONUS grid is obtained by stitching all the tiles together.

The NMQ computer cluster architecture uses a Linux operating system and consists of 10 nodes with 2 CPU processors per node. Each CPU processor is 3.2 GHz in speed and has 3GB RAM. Among the 10 computer nodes, 4 are used for single radar pre-processing and 6 are used for spherical to Cartesian remapping and mosaicing. Figure 3 illustrates the network infrastructure of the NMQ mosaic system.

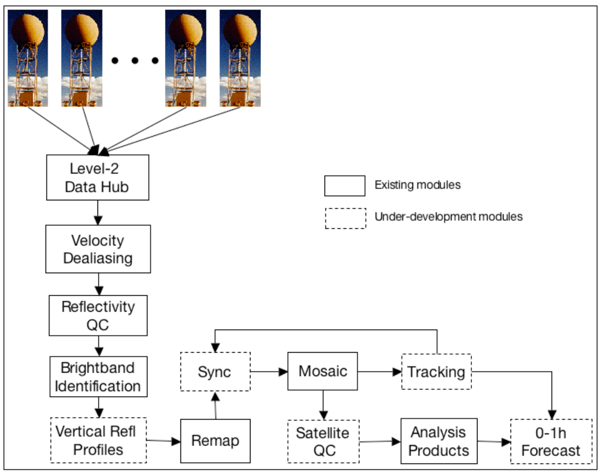

Fig. 1 An overview flowchart of the NMQ 3D high-resolution radar mosaic system.

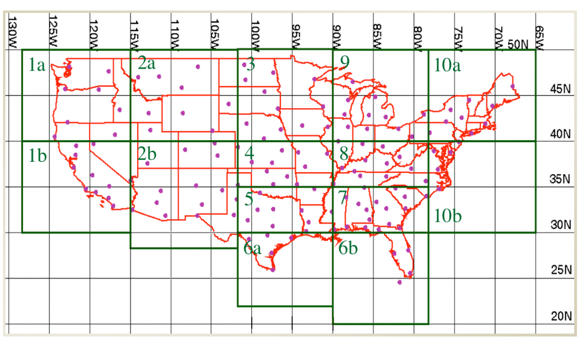

Fig. 2 The NMQ domain is divided into 14 individual sub-grids (or "tiles"). The sizes of the tiles are determined by precipitation climatology and radar station density.

3 SINGLE RADAR VOLUME SCAN DATA PROCESSING

3.1 Radial alignment

The level-2 data are saved in spherical coordinates of r, ϕ, θ, where r is the slant range, ϕ is azimuth angle from North, and θ is elevation angle from the horizontal. Data spacing along the radial direction (Δr) is constant (e.g., 1 km for reflectivity and 250 m for radial velocity). The data spacing between adjacent radials in azimuthal direction ($\Delta\phi$) is approximately 1° but it is variable. To simplify bookkeeping procedure of the data and to increase computational efficiencies, azimuth angles of each observational radial are rounded to whole degrees such that the data are organized onto a regular 1 km × 1° spherical grid. For radial velocity, the resolutions can be set to 250 m × 1°. The resolutions of the spherical grid are adaptive parameters, and can be increased to utilize higher resolution data sets.

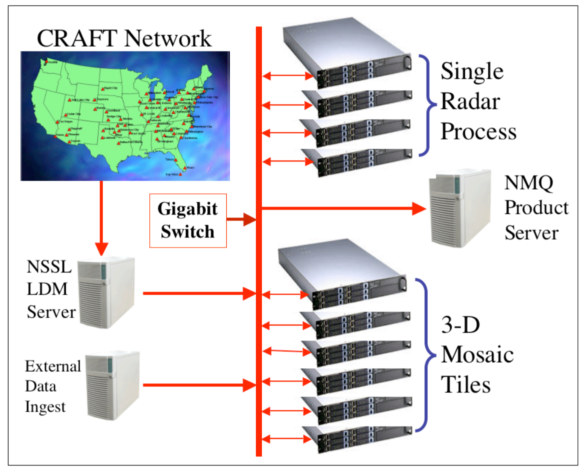

Fig. 3 Illustration of the network infrastructure for the NMQ 3D mosaic system.

3.2 Reflectivity quality control (QC)

The purpose of the reflectivity QC is to remove non-meteorological echoes such as ground and sea clutter due to normal and anomalous propagations (AP), biological targets including birds and insects, and electronic interferences. The QC algorithm are based on the following physical conventions and/or observations:

1) Biological targets are mostly below 3-4 km above radar level (ARL);
2) Meteorological targets have some vertical continuity. The stronger the targets (echoes) at the lower level, the larger the vertical scale of the echoes should be;
3) Most of the clear air and insects echoes are associated with small-scale noise that does not exist in meteorological echoes.

A detailed description of the complexities associated with the QC algorithm is beyond the scope of this paper. However, an example of the reflectivity QC 'before and after' results are shown in Fig. 4. Figure 4a shows a case where stratiform precipitation is seen to the east of the radar and echoes attributed to birds surround the radar behind the precipitation region. The precipitation echoes are relatively deep (echo top > 5 km). The QC algorithm successfully removed the bird echoes (Fig. 4b) with the vertical continuity criteria playing the decisive role in removing the non-meteorological echoes.

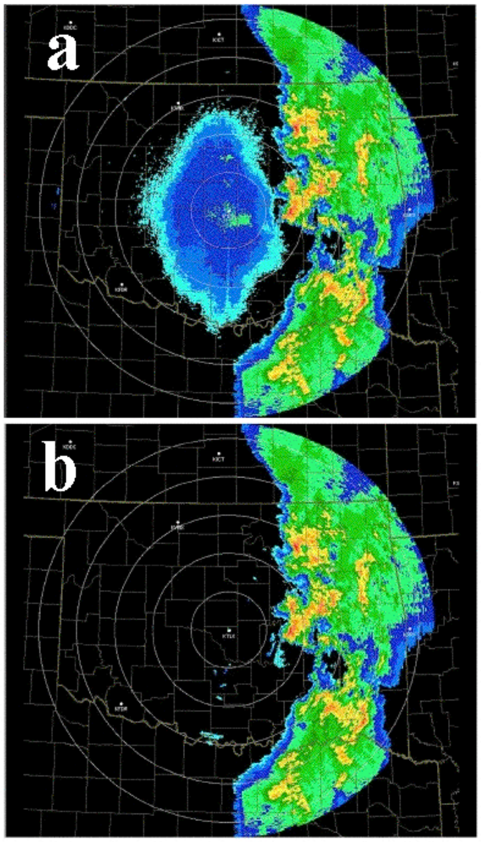

Fig. 4 Example base reflectivity images from 0.5° tilt before (a) and after (b) the reflectivity QC. The observations are from the KTLX (Twin Lakes, Oklahoma) radar at 0704 UTC on 4 May 1999. The reflectivity QC successfully removed the birds echoes surround the radar behind a stratiform precipitation region to the east of the radar.

3.3 Bright-band identification

Bright-band is an enhanced reflectivity layer associated with melting hydrometeors around the 0°C level (Atlas and Banks 1950). Identifying existence of a bright-band is necessary for understanding the 3D structure of the observed precipitation systems and for a more representative 3D analysis of reflectivity field. An automated bright-band identification algorithm developed by Gourley and Calvert (2000) is employed in the NMQ 3D mosaic system.

3.4 Transformation from spherical to Cartesian coordinates

After quality control, volume scans of reflectivity data from individual radars are remapped from the native spherical coordinates onto a common 3D Cartesian grid. The analysis scheme include nearest neighbor in range and azimuth directions and linear interpolations between the elevation angles. If no bright-band is detected, then a vertical interpolation between elevation angles is performed where analysis value at any given grid point (e.g., “A” in Fig.5) is obtained by linearly interpolating two observations at the same range as the grid point from the two tilts above and below the grid point. If a bright-band is identified, then an additional horizontal interpolation is performed for grid points in the gaps between the higher tilts and near the bright-band layer (e.g., “B” in Fig. 5) using two observations at the same height as the grid point and from the two tilts below and above the grid point. The additional horizontal interpolation is needed for filling in large gaps between the higher tilts of WSR-88D scans that result in poor horizontal sampling of the bright-band layer. Without the horizontal interpolation, ring-shaped artifacts centered at the radar often show on horizontal cross sections of reflectivity analyses at heights of near the bright-band layer (Zhang et al., 2001, 2003).

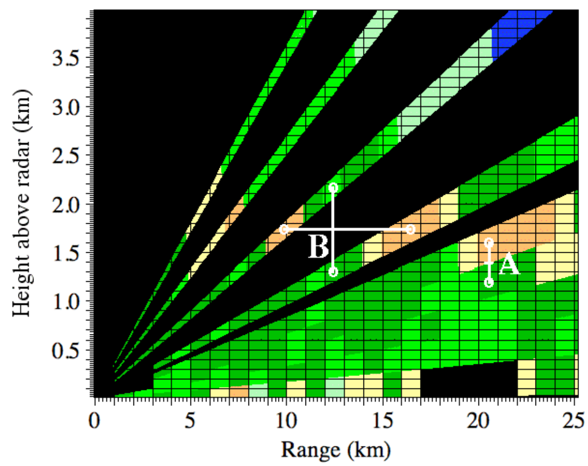

Fig. 5 An illustration of the horizontal and the vertical interpolation schemes on a RHI (range-height indicator) plot. The shaded areas represent reflectivity observation gates in radar beams and the thin black lines show constant range and height lines at 1 km × 100 m interval. The vertical interpolation scheme is illustrated at a grid point “A” and the additional horizontal interpolation is illustrated at a grid point “B”.

4 MULTIPLE RADAR MOSAIC

4.1 3D Mosaic

Once reflectivity data from all radars are mapped from their native spherical coordinates onto the common Cartesian grid, remapped reflectivity values (from all radars) at any given grid cell in the Cartesian grid are combined via a weighted average scheme to produce the final mosaic value at the grid point. The weighting for each remapped reflectivity value is a function of the distance between the grid cell to the radar associated with the remapped reflectivity value. Currently the following exponential weighting function is used in the national 3D mosaic:

$$W = \exp\left[-\frac{d^2}{L^2}\right] \quad (1)$$

Here W is the weight, d is the distance, and L is a constant length scale with a default value of 50 km.

An example NMQ composite reflectivity is shown in Fig. 6a. The mosaic field is consistent and seamless across umbrellas of different radars and across boundaries of the tiles. This example was from the very first 1-km NMQ mosaic product using level-2 data from 130 radars in real-time. The zoomed-in images (Figs. 6b and 6c) show detailed structure of storms in smaller regions. Several 2D products, such as vertically integrated liquid, severe hail index, etc, are currently derived from the 3D grid.

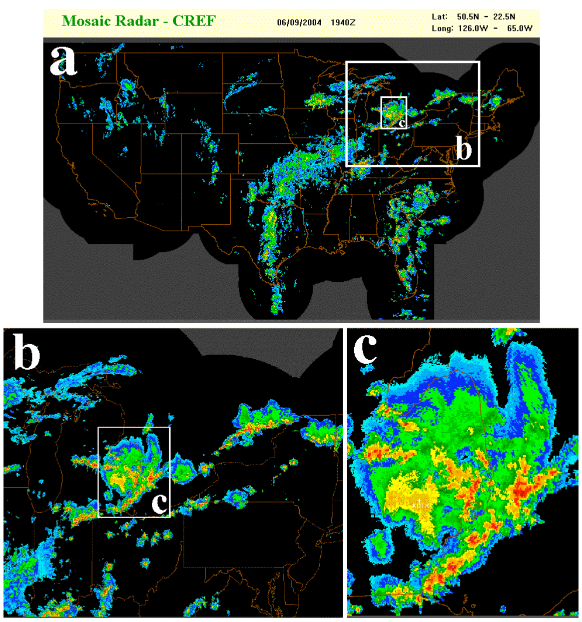

Fig. 6 An example composite reflectivity image from the NMQ 3D mosaic (a) and two zooming-in images for smaller regions (b and c).

4.2 Computational performance

The 3D high-resolution national mosaic has been running in real-time at the NSSL since June 2004. The performance of the NMQ 3D mosaic system has been closely monitored. A NMQ system monitoring web page (http://nmqserver.nssl.noaa.gov/~qpeverif/) has been instituted and performance statistics are displayed within the web page. The statistics include latencies of each process, radar data networking status, percentage of echo coverage, etc. Example plots of the performance statistics are shown in Figs. 7 and 8. Figure 7 shows time series of 1) radar VCPs (panel a); 2) latency of level-2 data over the network from a radar site to the NSSL NMQ system (panel b); 3) total clock time for running single radar processes (i.e., alignment, reflectivity QC, velocity dealiasing, etc) (panel c); and 4) percentage area with -30dBZ or higher echoes in the first tilt of radar volume scan within the 460 km radar umbrella (panel d). Two small data gaps are apparent around 08:45 and 10:45 UTC. Figure 8 shows performance statistics for the 3D mosaic process in a tile. The plots include time series of 1) clock and CPU times for each mosaic run (panel a); 2) number of radars went into the mosaic run (panel b); and 3) percentage area with -30dBZ or higher echoes in the tile (panel c).

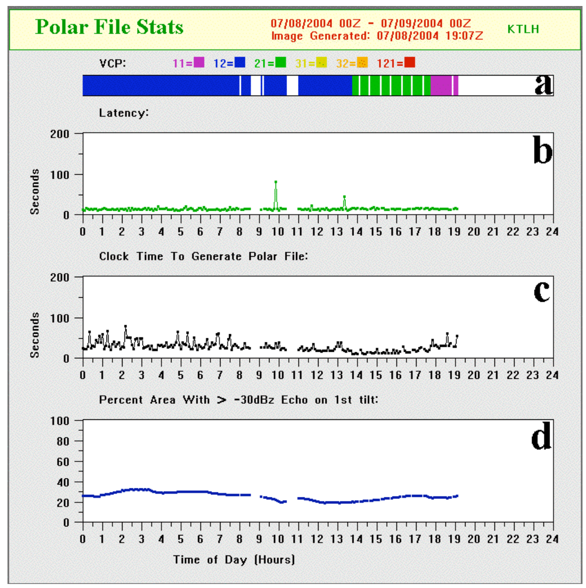

Fig 7 Example plots of performance statistics for a single radar processing. The plots show time series of (a) radar VCPs, (b) latency of level-2 data networking between the radar site and the NMQ system, (c) total clock time for running all single radar processes (i.e., alignment, reflectivity QC, velocity dealiasing, etc), and (d) the percentage area with –30dBZ or higher echoes in the 460 km radar umbrella. Two small data gaps are apparent around 08:45 and 10:45 UTC.

During a three-week test period, the NMQ mosaic software system has shown to be very stable and computationally efficient. Utilizing only 6 nodes, the NMQ can produce the 1-km resolution national 3D mosaic every 5 minutes more than 90% of the time. The latency of the mosaic products (from ending time of volume scans to ending time of the 3D mosaic grid generation) is less than 15 minutes more than 90% of the time.

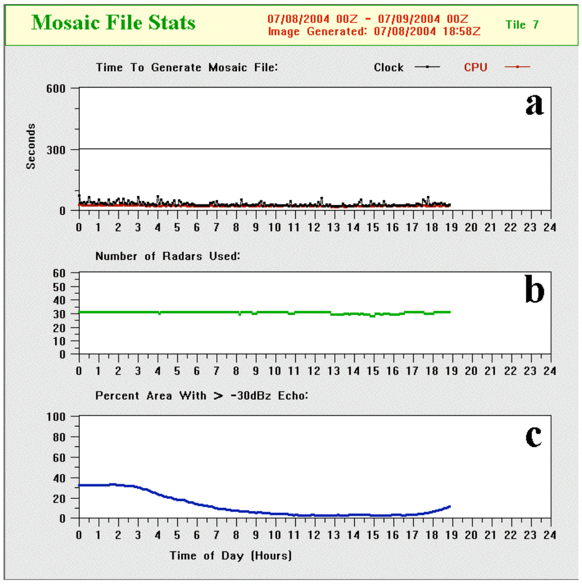

Fig 8 Example plots of performance statistics for the 3D mosaic process in tile 7. The statistics include time series of (a) clock and CPU times for running the 3D mosaic for the tile, (b) number of radars went into the mosaic, and (c) the percentage area with -30dBZ or higher echoes in the tile. Note that the mosaic runs every 5 minutes.

5 RESULTS AND SUMMARY

A national 3D radar reflectivity mosaic system is introduced in this paper. The system includes components that perform reflectivity quality control, 3D spherical to Cartesian grid transformation, and weighted mean multiple radar reflectivity mosaic. The NMQ 3D mosaic is consistent and seamless while successfully retaining the high-resolution storm structure that is apparent in the raw radar observations. Real-time implementation and testing has shown that the NMQ 3D mosaic system is stable and computationally efficient to reside as part of an operational system. The 3D grid can be useful for derived products such as high-resolution rainfall maps, severe storm identification products, hazardous weather products for aviation, and for data assimilations in convective scale numerical weather prediction models.

Undergoing development efforts include synchronization of the reflectivity volume scans valid at different times in the 3D mosaic (Fig. 1). New gap-filling techniques, such as the vertical profile of reflectivity (VPR), are currently under development and testing. These gap-filling techniques can be helpful in filling in the radars “cone of silence” in addition to data void below the lowest radar beams due to the earth curvature. Satellite imagery data will be used to help further enhancing the reflectivity QC. Data from other radars, e.g., the Federal Aviation Administration’s (FAA) Terminal Doppler Weather Radar (TDWR), will be integrated into the national 3D mosaic. A 0-1h storm and precipitation forecast based the national mosaic will be developed.

Future work will also include development of a 4D radar mosaic grid that updates based on the time scales of an individual tilt instead of the time scales of a volume scan. The 4D radar mosaic technique will be suitable for the analysis of rapid update radar such as phased array radars. The rapid update NMQ 4-D mosaic can provide users, especially those from the aviation community, more recent information of storm structure and distribution than the 3D mosaic. The most up-to-date storm data are very important for hazardous weather forecasts and warnings and for saving property and lives.

Acknowledgements

Major funding for this research was provided under the Aviation Weather Research Program NAPDT (NEXRAD Algorithms Product Development Team) MOU and partial funding was provided under NOAA-OU Cooperative Agreement #NA17RJ1227 and through the collaboration with the Central Weather Bureau of Taiwan, Republic of China.

This research is in response to requirements and funding by the Federal Aviation Administration (FAA). The views expressed are those of the authors and do not necessarily represent the official policy or position of the FAA.

References

Atlas, D, and H. C. Banks, 1950: A virtual echo-layer above the bright band**.** *J. Atmos. Sci.,* **7,** 402–403.

Gourley, J.J. and C.M. Calvert, 2003: Automated detection of the bright band using WSR-88D radar data. *Wea. Forecasting*, **18,** 585-599.

Zhang, J., K. Howard, W. Xia, and J.J. Gourley, 2003: Comparison of Objective Analysis Schemes for the WSR-88D Radar Data. *Preprints, The 31th Conference on Radar Meteorology*. 5-12 August 2003, Seattle, Washington, 907-910.

Zhang, J., J. J. Gourley, K. Howard, and B. Maddox, 2001: Three-dimensional gridding and mosaic of reflectivities from multiple WSR-88D radars. *Preprints, The 30th International Radar Conference,* 19-24 July 2001, Munich, Germany, 719-721.